



**HAL**  
open science

# The role of three-dimensional bulk clusters in determining surface morphologies of intermetallic compounds:

É. Gaudry, J. Ledieu, V. Fournée

► **To cite this version:**

É. Gaudry, J. Ledieu, V. Fournée. The role of three-dimensional bulk clusters in determining surface morphologies of intermetallic compounds:: Quasicrystals to clathrates. *Journal of Chemical Physics*, 2021, 154 (12), pp.124706. 10.1063/5.0038103 . hal-03317134

**HAL Id: hal-03317134**

**<https://hal.science/hal-03317134>**

Submitted on 21 Oct 2021

**HAL** is a multi-disciplinary open access archive for the deposit and dissemination of scientific research documents, whether they are published or not. The documents may come from teaching and research institutions in France or abroad, or from public or private research centers.

L'archive ouverte pluridisciplinaire **HAL**, est destinée au dépôt et à la diffusion de documents scientifiques de niveau recherche, publiés ou non, émanant des établissements d'enseignement et de recherche français ou étrangers, des laboratoires publics ou privés.

# The role of three-dimensional bulk clusters in determining surface morphologies of intermetallic compounds: Quasicrystals to clathrates

Cite as: J. Chem. Phys. **154**, 124706 (2021); <https://doi.org/10.1063/5.0038103>

Submitted: 18 November 2020 • Accepted: 08 March 2021 • Published Online: 24 March 2021

 É. Gaudry,  J. Ledieu and  V. Fournée

## COLLECTIONS

Paper published as part of the special topic on [Special Collection in Honor of Women in Chemical Physics and Physical Chemistry](#)



View Online



Export Citation



CrossMark

## ARTICLES YOU MAY BE INTERESTED IN

[Computational studies of the electronic structure of copper-doped ZnO quantum dots](#)

The Journal of Chemical Physics **154**, 124710 (2021); <https://doi.org/10.1063/5.0039522>

[The Li-F-H ternary system at high pressures](#)

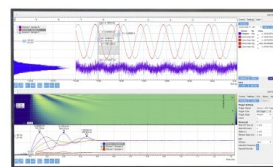
The Journal of Chemical Physics **154**, 124709 (2021); <https://doi.org/10.1063/5.0041490>

[Describing adsorption of benzene, thiophene, and xenon on coinage metals by using the Zaremba-Kohn theory-based model](#)

The Journal of Chemical Physics **154**, 124705 (2021); <https://doi.org/10.1063/5.0042719>

Challenge us.

What are your needs for  
periodic signal detection?



Zurich  
Instruments

# The role of three-dimensional bulk clusters in determining surface morphologies of intermetallic compounds: Quasicrystals to clathrates

Cite as: J. Chem. Phys. 154, 124706 (2021); doi: 10.1063/5.0038103

Submitted: 18 November 2020 • Accepted: 8 March 2021 •

Published Online: 24 March 2021



View Online



Export Citation



CrossMark

É. Gaudry,<sup>a)</sup>  J. Ledieu,  and V. Fournée 

## AFFILIATIONS

University of Lorraine, CNRS, IJL, F-54000 Nancy, France

**Note:** This paper is part of the JCP Special Collection in Honor of Women in Chemical Physics and Physical Chemistry.

<sup>a)</sup>Author to whom correspondence should be addressed: [Emilie.Gaudry@univ-lorraine.fr](mailto:Emilie.Gaudry@univ-lorraine.fr)

## ABSTRACT

Nanostructured alloy surfaces present unique physical properties and chemical reactivities that are quite different from those of the close-packed low-index surfaces. This can be beneficial for the design of new catalysts and electronic and data-storage devices. However, the growth of such surface nanostructures is not straightforward at the atomic scale. The cluster-based bulk structure of intermetallic compounds presents an original alternative to build surfaces with specific morphologies, in comparison to more traditional methods based on mechanical, chemical, or plasma treatments. It relies on their specific electronic structures—built from a network of bonds with a combination of ionic, covalent-like, and metallic characters, and also depends on the experimental conditions. In this paper, a few surface structures of cluster-based intermetallics are reviewed, with a special emphasis on quasicrystals and clathrates. We show how the intrinsic electronic properties of such compounds, as well as the surface preparation conditions, impact their surface morphologies, which can further influence the growth of atomic and molecular thin films at their surface.

Published under license by AIP Publishing. <https://doi.org/10.1063/5.0038103>

## INTRODUCTION

Most of the close-packed metal low-index surfaces observed under ultrahigh vacuum (UHV) conditions are bulk truncated flat planes separated by atomic steps.<sup>1,2</sup> Exceptions are the surfaces of a few 5d-transition metals that reconstruct to increase the packing density<sup>3–7</sup> or the surfaces that suffer from roughening and faceting.<sup>8</sup> Great efforts are taken to control the metallic surface structures and morphologies, with the aim to enhance their properties for a wide range of applications, such as wetting,<sup>9</sup> plasmonic behavior,<sup>10</sup> or chemical reactivity.<sup>11,12</sup> The search for metallic nanostructured surfaces, which represents one of the most promising practical low-cost approaches for nanofabrication, requires, then, to adopt specific strategies.

For several years, mechanical, chemical, or plasma treatments have been used to tune the surface roughness of metals. Overlayers or thin films, grown at the surface, can modify not only

the surface morphologies but also their functionalities.<sup>13,14</sup> Strongly corrugated monolayers of sp<sup>2</sup>-bonded materials, such as hexagonal boron nitride (h-BN) and graphene,<sup>15,16</sup> formed on lattice-mismatched transition metal substrates, provide interesting potential energy landscapes. The strategy that consists in taking advantage of the intrinsic structural and electronic properties of the metallic materials to design a nanostructured surface is less frequent. It relies on the observation that most of the intermetallic crystal structures are based on polyhedral entities. According to the statistical and topological investigations of the crystal structures displayed by the 38 000 intermetallic compounds gathered in the Inorganic Crystal Structure Database (ICSD)<sup>17</sup> and Pearson's Crystal Data,<sup>18</sup> 12-vertex polyhedra are the most frequent (33%) and almost half of them are icosahedron-like (46%).<sup>19</sup>

Cage-like compounds have attracted strong interest in the last few years due to their potential industrial applications in diverse fields such as gas storage<sup>20,21</sup> or thermoelectric

applications.<sup>22</sup> Focusing on surfaces, the question arises about the role of three-dimensional bulk polyhedra in determining surface morphologies. This fundamental question—also linked to the question of the physical or chemical nature of the building blocks, which is not revealed by the previous statistical analysis—is also related to applications because the surface morphology has a non-negligible influence on several surface properties.

In this paper, we focus on a few cluster-based intermetallic compounds, from quasicrystals to clathrates. Several reviews have already addressed the topic of complex intermetallic or quasicrystalline surface structures these last years.<sup>23–25</sup> Here, we put the emphasis on phases belonging to the family of cage compounds. Their bulk structure can be described by three-dimensional (3D) frameworks of host atoms forming cages. Their surface morphology generally strongly depends on the chemical potentials, i.e., on the surface preparation and on the exact composition of the single crystalline ingot used for the experiments (number of vacancies, anti-sites, etc.).<sup>26,27</sup> The investigation of the role of bulk clusters in surface morphologies requires detailed determinations of surface structures, usually through combinations of experimental and theoretical methods. Electronic and structural determinations on the basis of a single surface science technique, such as photoemission spectroscopy, low energy electron diffraction (LEED), surface x-ray diffraction (SXR), or scanning tunneling microscopy (STM), are often a challenge because they are indirect methods to probe the surface atomic structure. Optimizations involving a large number of parameters are required to fit LEED or SXR data, while STM reveals the surface electronic structure.

On the other hand, theoretical methods, often based on Density Functional Theory (DFT), can compare the thermodynamic stability of different structural models but lack the experimental observations. Combining both approaches, by theoretical simulations of STM images, SXR rods, or dynamical LEED, usually leads to reliable results. Three important aspects of the interaction between the 3D bulk structure and the 2D surface are detailed in the following: how the electronic properties of intermetallic compounds impact its surface morphologies, what is the influence of the experimental conditions (preparation and operating conditions) on the surface morphologies, and how the surface structures of cluster-based intermetallic compounds can be used to grow molecular and atomic thin films with specific surface morphologies.

## HOW THE ELECTRONIC PROPERTIES OF INTERMETALLIC COMPOUNDS IMPACT THEIR SURFACE MORPHOLOGIES

The observation of a specific termination at complex intermetallic surfaces is driven by the minimization of the surface energy, i.e., the excess energy at the surface in comparison to bulk. It depends on the bond network and the cohesive energy of the solid. Indeed, the stronger the bonds in the compound, the more expensive it is to break them and, therefore, to create a surface. In turn, the higher is the surface energy. Thus, the intrinsic electronic properties of intermetallic compounds play a decisive role in the occurrence of specific morphologies at their surfaces.

The range of electronic structures exhibited by intermetallic cage compounds is rather large, from compounds with a metallic character to semiconducting ones. In several ordered alloys,

the electronic structure can be understood within the (nearly) free electron model, leading to specific composition-averaged valence according to the Hume–Rothery electron concentration rule. The electronic energy is minimized for a specific  $e/a$  (electron per atom) ratio, thanks to the formation of a pseudo-gap in the electronic density of states.<sup>28</sup> Experimentally, the magnitude of the pseudogap, related to the interaction of the Fermi sphere with the Brillouin zone boundary, was found to critically depend on the periodicity. It has been demonstrated by the measurement of the Hume–Rothery gap for the periodic and quasiperiodic directions of the decagonal Al–Ni–Co quasicrystal, using soft x-ray angle-resolved photoemission spectroscopy.<sup>29</sup> In other types of compounds, containing elements with rather different electronegativities, charge transfers occur so that the most electronegative elements either use those electrons to form a closed-shell ion or, if there are not enough electrons for this, to form bonds in order to achieve a full octet of electrons. Between these two limit cases, polar intermetallics exhibit a network of bonds with a combination of ionic, covalent-like, and metallic characters. In the following, several examples are presented, in relation to their intrinsic electronic properties.

## Bulk cage Hume–Rothery compounds

Hume–Rothery compounds include structures of different complexities ranging from the simple close-packed to the more complex  $\gamma$ -brasses<sup>30</sup> and quasicrystals.<sup>31,32</sup> In the following, we focus on  $\gamma$ -brass solids, which can be viewed as a collection of  $3 \times 3 \times 3$  CsCl units including two vacancies.<sup>33,34</sup> The  $\gamma$ -brass structures can also be described as a bcc arrangement of 26-atom polyhedra,<sup>35</sup> made of concentric inner tetrahedral, outer tetrahedral, octahedral, and cubo-octahedral polyhedra [red, green, orange, and blue clusters in Fig. 1(a)]. While surface structure investigations of the most simple alloys are quite common, the studies of the atomic arrangement at the surface of  $\gamma$ -brass compounds are rather scarce. To our knowledge, attempts in this direction are limited to the Ni–Zn and Al–Cu  $\gamma$ -brass phases.<sup>36–38</sup>

As a Hume–Rothery compound,<sup>28</sup> with a valence electron per unit volume ( $0.127e/\text{\AA}^3$ ) close to that of the icosahedral  $i$ -AlCuFe phase ( $0.124e/\text{\AA}^3$ ),<sup>39</sup> Al<sub>4</sub>Cu<sub>9</sub> can be considered as a prototype for non-polar Al-based quasicrystalline approximants. Focusing on the oriented (110) single crystal surface, two types of terminations have been revealed experimentally under UHV,<sup>36,37</sup> using a surface prepared by cycles of sputtering and annealing. Theoretical calculations based on DFT identified two possible terminations, built by bulk truncation and selection of dense planes at the surface. Their surface energies are very similar (within 0.06 J/m<sup>2</sup>). The corresponding simulated STM images are in reasonable agreement with the experimental ones and mirror the experimental voltage dependence. The two terminations differ by their surface composition and by the fact that only one of the two cuts the inner tetrahedra. Such a surface morphology leads to a rather small surface corrugation (0.6–0.7 Å), in agreement with the general trends observed for related quasicrystalline phases. Similarly to what occurs in alloy surfaces, a weak segregation, i.e., a weak enrichment of the surface in one of the components in comparison to the bulk concentration, seems to take place at this surface. In this case, the role of the three-dimensional cages on the surface morphology is negligible.

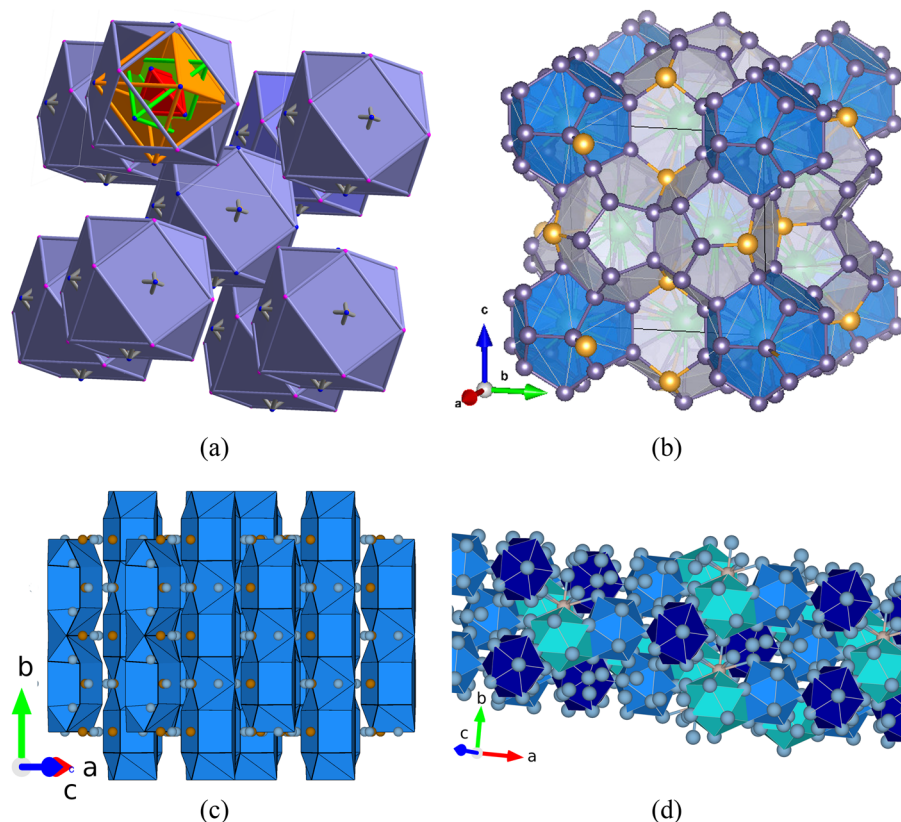


**FIG. 1.** Bulk structure of several cage compounds: (a)  $\gamma$ - $\text{Al}_4\text{Cu}_9$ , (b)  $\text{Ba}_8\text{Au}_{5.25}\text{Ge}_{40.75}$ , (c)  $\text{Al}_{13}\text{Fe}_4$ , and (d)  $\text{Al}_{45}\text{Cr}_7$ .

The  $\gamma$ -brass compounds can also be prepared as nanoparticles of rather small size ( $<10$  nm).<sup>40</sup> Simple probe reactions can be used in that case to characterize their surfaces as catalytic kinetics are directly affected by the surface properties. This indirect method has been applied to the Ni–Zn  $\gamma$ -brass,<sup>38</sup> using several compounds with different Ni contents. Two chemical reactions were considered—hydrogen–deuterium exchange and ethylene hydrogenation. The insensitivity of the catalytic performances to the considered sample was attributed to the absence of Ni trimer sites at the surface. Thus, it excludes the presence of the  $\{110\}$  planes at the surface of the nanoparticle, according to the authors.

In summary, the interaction of the 3D bulk structure and the 2D surfaces is expected to lead to rather flat surface morphologies for Hume–Rothery  $\gamma$ -brass compounds, large cages predicted to be broken at the surface. This conclusion is in agreement with the general trends observed for quasicrystalline surfaces, although the degree of complexity of the  $\gamma$ -brass phase, set by the number of atoms per unit cell, is sensibly lower.

### Zintl clathrates

Zintl clathrates are a vast family of cage compounds whose structure can be described by a rigid network of covalently bonded atoms, consisting of large polyhedral cages. The most common polyhedron is the 20-vertex pentagonal dodecahedron, which contains fivefold symmetry axes and, thus, is combined with polyhedra of other types to build a 3D periodic structure.

Surface science studies on intermetallic clathrate surfaces are very scarce. A nanosized layer of phosphorus-doped silica has been revealed by X-ray Photoelectron Spectroscopy (XPS) at the surface of the type III Si–P–Te clathrate,<sup>41</sup> with a sample heat-treated in air at 1273 K. When the surface is prepared under UHV, by cycles of sputtering and annealing, no oxide layer is formed, as demonstrated with the type I Ba–Au–Ge clathrate low-index surfaces.<sup>42,43</sup> In the following, we focus on the latter compound whose bulk structure consists of a rigid framework of  $sp^3$  bonded Ge and Au atoms, with Ba atoms in the center of the cages.

Surface nanostructuring of Zintl clathrates is expected with intact cages at the surface. It has been evidenced by the structure investigations of the low index—(100) and (110)—surfaces of Ba–Au–Ge, a Zintl compound made of two types of cages [tetrakaidecahedra and dodecahedra, Fig. 1(b)]. In both cases, the termination contains low coordination surface Au and Ge ( $sp^2$ ) atoms. An ordered arrangement of Ba cations at the surface, located in the center of the cages, which were dissected following the bulk truncation process, contributes to the surface stabilization. It proceeds through a passivation of the dangling bonds by a charge transfer from the electropositive surface Ba atoms to the neighboring electronegative Ge and Au atoms, similarly to what occurs on semiconductor surfaces.<sup>44,45</sup> The surface orientation—(100) or (110)—controls the surface nanostructuring of the Ba–Au–Ge clathrate by the selection of cages at the surface: tetrakaidecahedra clusters (with 12 pentagonal faces and two hexagonal faces) at the (100) surface and dodecahedra (with 12 pentagonal faces) at the (110) surface. In both cases, the

surface corrugation is rather high ( $\approx 2 \text{ \AA}$ ) and depends on the size of the cages in the bulk compound.

### Binary Al-TM quasicrystalline approximants

Most of the Al-TM (TM = transition metal) quasicrystalline approximants belong to the family of polar intermetallics. The bonding network of these compounds presents a covalent-like, ionic, and metallic character,<sup>46–49</sup> thus giving rise to a large variety of structures. At the surface, the range of structures is even wider because of the different possible surface orientations.

Surface investigations of Al-based polar intermetallics include the  $\text{Al}_5\text{Co}_2$  low index surfaces,<sup>50,51</sup> the pseudo-tenfold surfaces of  $\text{Al}_{13}\text{TM}_4$  (TM = Co, Fe, and Ru) binaries [Fig. 1(c)],<sup>52–56</sup> and  $\text{Al}_{45}\text{Cr}_7(010)$  [Fig. 1(d)]. The previous Al-TM compounds present a cluster-based structure with characteristic features of pseudo-icosahedral symmetry, with the exception of  $\text{Al}_5\text{Co}_2$  for which pentagonal atomic arrangements are present in the bulk but without such symmetry for the atomic polyhedra. They all also show a bulk structure described as a stacking of at least two types of planes. Rather flat terminations are predicted for  $\text{Al}_{45}\text{Cr}_7(010)$ , according to surface energy calculations.<sup>57</sup> A similar conclusion was drawn for  $\text{Al}_{13}\text{Co}_4(100)$ , prepared by cycles of sputtering and annealing, under UHV, according to a combination of surface science studies and DFT-based calculations.<sup>53,54</sup> It means that in both cases, the surface terminations consist of truncated clusters. In contrast, the surface morphology of  $\text{Al}_{13}\text{Fe}_4(010)$  is highly corrugated, the clusters of the bulk being kept intact at the surface,<sup>52</sup> while  $\text{Al}_{13}\text{Ru}_4(010)$  shows a surface morphology characterized by an atypical surface reconstruction with the occurrence of pentagonal motifs and vacancies.<sup>56</sup> It is worth noting that the surface morphologies here strongly depend on the surface orientation, as demonstrated by the faceted and columnar structures of  $\text{Al}_{13}\text{Co}_4(010)$ .<sup>58</sup>

Rationalizing the diversity of surface structures described in the previous paragraph is not straightforward. Attempts have been made based on the Crystal Orbital Hamilton Population (COHP) method to evaluate the strength of the typical bonds that ensure the cohesion of the cages. In  $\text{Al}_{13}\text{Co}_4$  and  $\text{Al}_{45}\text{Cr}_7$ , the averaged integrated COHPs of the typical Al–Co and Al–Cr bonds, which support the cages, are calculated to be 1.6 eV/bond,<sup>48,57</sup> i.e., weaker than the Al–Fe and Al–Ru bonds in  $\text{Al}_{13}\text{Fe}_4$  (1.8 eV/bond) and  $\text{Al}_{13}\text{Ru}_4$  (2.3 eV/bond).

This may explain the different behavior between the compound's surfaces.

In summary, several surface morphologies can be observed, from rather flat terminations to nanostructured ones. Overall, structures made with metallic elements lead to rather flat surfaces, while rigid networks made of Ge, for example, keep intact the cages at the surface. The case of  $\text{Ce}_3\text{Pd}_{20}\text{Si}_6(100)$  is intermediate, with complete  $\text{Pd}_{12}\text{Si}_6$  polyhedra at the surface, but with additional Pd surface atoms between the cages, lowering the surface corrugation.<sup>59</sup>

### HOW THE OPERATING CONDITIONS IMPACT THE SURFACE MORPHOLOGIES

Experimental investigations under UHV conditions usually require well-oriented single crystal surfaces that need to be cleaned to remove the oxide and carbonaceous species adsorbed due to air exposure prior to inserting the sample in the UHV system. Sometimes, this can be achieved by cleaving the sample *in situ*, such as to create a pristine surface, which can be analyzed immediately after. This method is pretty straightforward but has many drawbacks: it is sample consuming, the samples should be brittle enough to cleave mechanically, and the resulting surface morphology may not be flat. Another method consists in sputtering the contaminated surfaces with energetic rare gas ions, followed by thermal annealing cycles to restore the surface atomic order. Sputtering and annealing cycles are repeated until a clean surface is obtained, with no traces of oxygen or carbon. The annealing temperature should be high enough to allow for atomic diffusion in order to restore the structural order, but it can also induce chemical segregation or preferential evaporation of some of the elements in the compound.

In the case of quasicrystals, both methods have been used, resulting in very different surface morphologies. Ebert *et al.* first investigated the surface morphology of icosahedral  $\text{AlPdMn}$  quasicrystalline samples cleaved perpendicular to a fivefold or twofold rotational axis [Fig. 2(a)].<sup>60,61</sup> STM images revealed a rough surface, which was interpreted as resulting from the propagation of the crack through the weakest bonds at the boundary between the cluster building blocks. It thus relies on the hypothesis of a special stability associated with the cluster units. The rough surface had a typical elementary cluster with a diameter of about 1 nm, attributed to the Mackay-type cluster units. It was also suggested that, as along

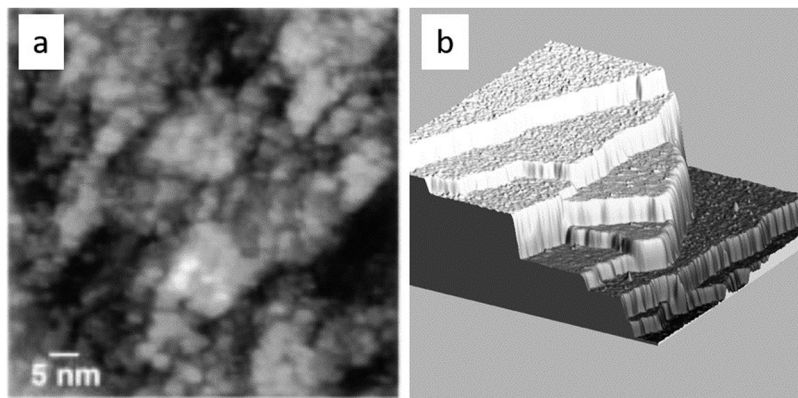


**FIG. 2.** (a) STM image of an *i*-AlPdMn quasicrystal cleaved perpendicular to a fivefold axis showing a clustered structure. Adapted from Ref. 60. (b) STM image ( $200 \times 200 \text{ nm}^2$ ) of an *i*-AlPdMn quasicrystal prepared by sputter-annealing methods showing a step-terrace morphology.

as surface phase transformations are excluded, the surface of quasicrystal should always be rough due to the arrangements of the cluster building blocks in the quasicrystal due to inter-cluster cleavage. This interpretation was later questioned as similar roughnesses have also been observed at the fracture surfaces of disordered and ordered materials.<sup>62</sup> Based on an analysis of the roughness statistical scaling properties using the same set of STM images, Ponson *et al.* concluded that the fracture surface roughness of quasicrystals obeys the same scaling behavior as many different types of materials. The nanoscale roughness could instead be interpreted as resulting from mechanical damages at the crack tip, and not as the signature of Mackay building blocks.

A contrario, quasicrystalline surfaces prepared by sputter-annealing cycles present a terrace-step morphology, similar to conventional crystals [Fig. 2(b)].<sup>63–67</sup> However, atomically flat terraces are separated by steps of unequal heights. The two smallest heights are related by the golden number, which is an irrational number. Other step heights are a linear combination of these two fundamental heights. In a conventional crystal, unequal step heights usually result from step bunching and are thus an integral number of a single fundamental step height. These particular step heights observed at quasicrystalline surfaces had been puzzling for quite some time. Indeed, it is known from bulk structural models that no two planes of atoms can be identical in a quasicrystal. Therefore, why should particular step heights be observed at all? Does it relate to the cluster building blocks and their spatial arrangement? The answer to this question came after a large number of investigations using different techniques including dynamical low-energy electron

diffraction, STM, helium atom scattering, medium and low energy ion scattering, and photoelectron diffraction. It is now accepted that quasicrystalline surfaces such as the fivefold surface of *i*-AlPdMn or *i*-AlCuFe model systems are bulk terminated. The specific step heights arise due to the selection of a specific set of bulk planes as surface terminations. The planes share specific characteristics: they are all chemically Al-rich and structurally dense planes. In the refined bulk structural models derived using x-ray diffraction data, relaxation of most atoms from their ideal position of geometric models leads to the emergence of blocks of atomic planes separated by larger gaps. The thicknesses of the blocks of atoms correspond to the observed step heights. Therefore, the planes selected as surface terminations are the Al-rich dense planes terminating these blocks of layers. High-resolution STM images of these planes reveal many features such as dark stars (DSs) and white-flower (WF) motifs [Fig. 3(a)]. The pentagonal star, for example, is identified as a Bergman cluster that is cut at its midpoint and is surrounded by other Bergman clusters hanging downwards into the bulk.<sup>68</sup> Therefore, some of the clusters' building blocks are truncated by the surface termination. It does not mean that the clusters do not play any role, but the energy associated with the formation of dense surface planes is larger than that associated with the preservation of the cluster integrity. Similar conclusions have been reached for different quasicrystalline systems such as the icosahedral AgInYb phase whose bulk structure is described by the packing of Tsai-type clusters.<sup>69</sup> Here also, low-index surfaces present a terrace-step morphology, and the surface terminations are identified as specific bulk planes that intersect the cluster building blocks.

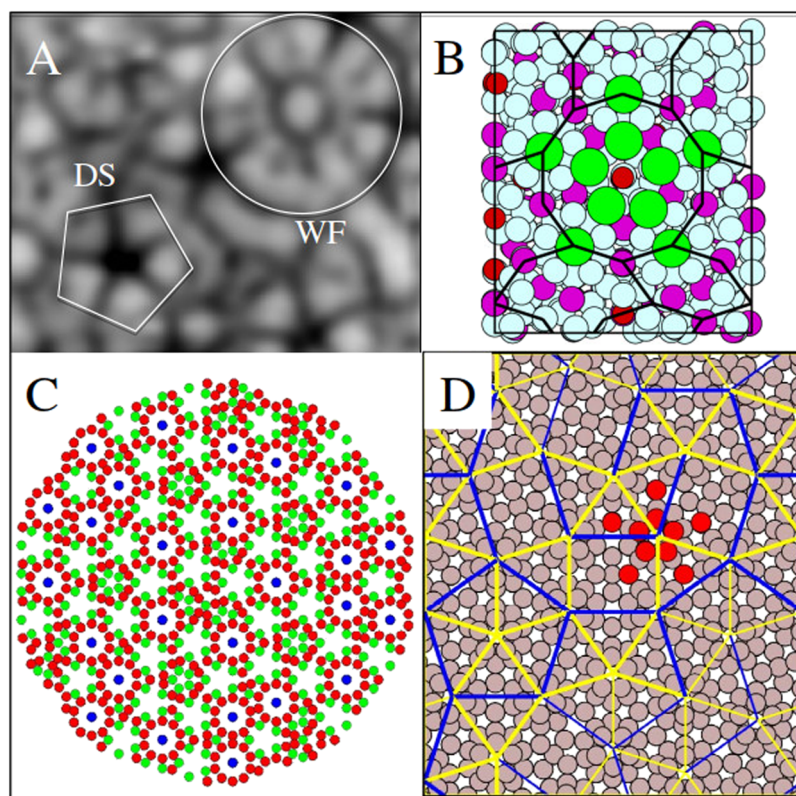


**FIG. 3.** (a) High resolution STM image showing the DS and WF motifs on the 5-*f* *i*-AlPdMn surface.<sup>84</sup> (b) Schematic representation of the ten-atom Pb starfish model made of pentagonal inner and outer rings (green spheres) grown on the quasicrystal surface.<sup>85</sup> (c) Structure of the 5-*f* *i*-AgInYb surface where green and red spheres correspond to Yb and Ag/In atoms, respectively.<sup>86</sup> (d) Representation of the quasicrystalline Sn clathrate atomic structure corresponding to the 5/3 approximant. The starfish cluster formed in the submonolayer regime upon adsorption of Sn on the 5-*f* *i*-AlPdMn surface is highlighted in the Sn structure.<sup>87</sup> [(a), (b), and (d)] are reprinted with permission from the American Physical Society. (c) is reprinted with permission from Springer Nature.

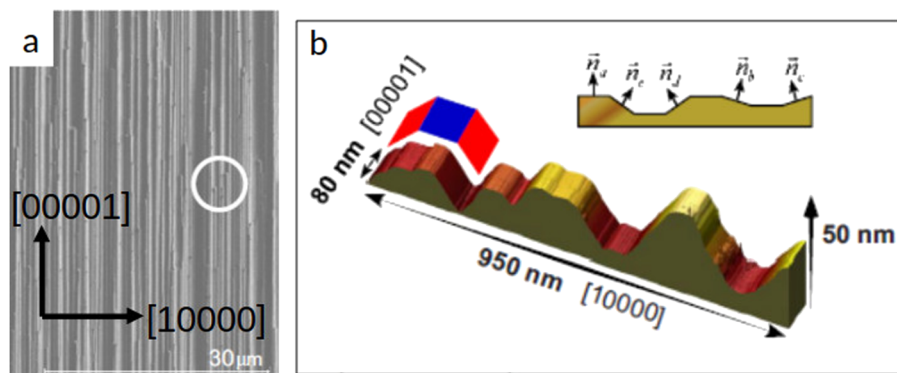


**FIG. 4.** (a) SEM image of the twofold (12 110) surface of d-AlNiCo showing the columnar structure motif extending along the tenfold axis. The white circle highlights an area of column endings. (b) 3D STM image representation of the d-AlNiCo (12 110) surface showing the faceting of the surface along the aperiodic direction (10 000), straight or blue for the (12 110) and inclined or red for the (10 000) facet, respectively. Adapted from Ref. 73.

We have seen that different surface preparation conditions lead to different surface morphologies. It also modifies the surface electronic structure, as evidenced by x-ray photoemission core level line shape analysis. Core level line shapes in metals are asymmetric due to electron–hole excitations across the Fermi level and the asymmetry parameter reflecting the electronic density of states at the Fermi level. In quasicrystals, the metal core levels become narrow and the asymmetry parameter is small due to the presence of a pseudogap in the electron density of states at the Fermi level. The pseudogap is not retained up to the surface immediately after fracture but can be restored by annealing or by sputter annealing the sample to sufficiently high temperatures.<sup>70–72</sup> Therefore, the surface preparation conditions also affect the surface electronic structure.

Some other quasicrystalline systems have shown some faceting upon surface preparation under UHV conditions. One example is the decagonal AlNiCo phase (Fig. 4).<sup>73,74</sup> Its structure consists of quasiperiodic planes, which are stacked periodically along the tenfold rotational [00001] axis. Alternatively, it can be described by decagonal columnar clusters having a diameter of 2 nm and extending along the [00001] direction that are located at the node of a pentagonal Penrose tiling.<sup>73</sup> In the quasiperiodic planes, there are two different types of twofold axes orthogonal to each other: [12 110] and [10 000]. Both types of two twofold surfaces contain a periodic and an aperiodic direction orthogonal to each other. They both display large and flat terraces with a columnar structure extending along the periodic direction. However, while the (10 000) surface remains flat, the (12 110) surface becomes faceted into (12 110) and (10 000) facets with a 1:1 area ratio. Atomic resolution STM images have been obtained, allowing to identify both types of terminations as a set of dense planes of the bulk structure, with some slight differences in surface chemistry and atomic densities.

A similar phenomenon has been observed in the orthorhombic crystalline approximant of the decagonal phase, the o-Al<sub>13</sub>Co<sub>4</sub> phase.<sup>58</sup> The structure of this crystal is also described by the packing of pseudo-decagonal clusters extending along the [100] pseudo-tenfold axis. A very closely related structure is the monoclinic approximant m-Al<sub>13</sub>Co<sub>4</sub>, in which the same pseudo-decagonal clusters are arranged in a slightly different manner. Both structures can coexist sometimes, giving rise to interface defects such as twins. The pseudo-twofold (010) surface of the o-Al<sub>13</sub>Co<sub>4</sub> phase has been investigated both experimentally and using DFT

calculations. It was found to display a columnar structure similar to that observed for the decagonal phase upon surface preparation. The columns extend along the [100] pseudo-tenfold axis. A surface model has been proposed consisting in the coexistence of flat o-Al<sub>13</sub>Co<sub>4</sub>(010) terraces and inclined facets of m-Al<sub>13</sub>Co<sub>4</sub>(201). The surface energies of the facets, determined through DFT calculations, are significantly lower than that of the flat o-Al<sub>13</sub>Co<sub>4</sub>(010) surface, and therefore, faceting is seen as a mechanism stabilizing the system. In this way, intrinsically nanostructured surfaces are obtained.

While the previous observation is strongly related to the presence of both monoclinic and orthorhombic phases, as well as extended defects in the bulk Al<sub>13</sub>Co<sub>4</sub>, such as twins, surface nanostructuring is also expected with surfaces exposed under hydroxylation reaction conditions. It is based on the fact that adsorbates can indeed strongly modify surface energies.<sup>75</sup> This has been demonstrated using the Al<sub>13</sub>Co<sub>4</sub>(100) surface as a model system. Hydrogen adsorption modifies the relatively flat surface structure identified under UHV, in the form of highly cohesive clusters emerging from the bulk lattice, thus leading to a nanostructured surface structure similar to the one of Al<sub>13</sub>Fe<sub>4</sub>(010).<sup>76</sup>

## HOW THE SUBSTRATE IMPACTS THE SURFACE MORPHOLOGIES OF THIN FILMS

In this section, few examples will be selected to demonstrate how the surfaces of the above described intermetallic compounds can impact thin film nucleation, growth, and *in fine* overall morphology (for comprehensive reviews on the adsorption and complex intermetallics, readers are referred to Refs. 77–80).

As explained above, the preparation of Hume–Rothery compounds under ultrahigh vacuum conditions generally leads to a relatively flat surface morphology.<sup>78,81</sup> For quasicrystals, the formation of a 2D surface implies dissecting highly symmetric clusters, basic building blocks of the 3D structure. The truncation of such structurally and chemically complex entities results in a unique potential energy landscape, with a rich variety of adsorption sites and with surfaces of various atomic densities. To illustrate this feature, we can consider the real space structure of *i*-AlCuFe and *i*-AlPdMn quasicrystals, which are built from interpenetrating Bergman (33 atoms) and pseudo-Mackay (51 atoms) clusters. Upon adsorption of Al atoms on the fivefold *i*-AlCuFe surface, the growth proceeds with the

formation of pseudomorphic islands, which resemble starfish.<sup>82</sup> The pentagonal DS sites have been identified as preferential nucleation sites. At low coverage, diffusing adatoms will be trapped at the center of such depressions and then stabilize five additional Al atoms in its periphery.<sup>82,83</sup> Once all DS sites become populated, a disordered 3D growth mode is observed, i.e., the starfish do not grow laterally.

Pentagonal islands have also been observed at the early stages of Pb and Bi nucleation on the fivefold *i*-AlPdMn surface.<sup>88,89</sup> Contrary to the previous system, the starfish are located atop WF sites [Fig. 3(b)]. Except for its fivefold symmetric shape, the WF site is also chemically unique as it is centered by a Mn atom. Upon adsorption of Pb atoms, a quasiperiodic monolayer is formed via self-assembly of an interconnected network of ten-atom Pb starfish.<sup>85,88</sup> Adatom–adatom interaction is key to stabilize the Pb starfish upon which the aperiodic film will grow. The adsorption of Bi atoms on the same quasicrystalline surface proceeds initially with the nucleation of pentagonal clusters on the WF site and then to the growth of a quasiperiodic overlayer. Contrary to the Pb adatom, each starfish is composed of five adatoms (only the inner ring). The high density of WF is sufficient to build a quasiperiodic framework,<sup>89</sup> the remaining gaps (less energetically favorable adsorption sites) being filled by impinging adatoms. Once complete, the corrugation of the overlayer is three times higher than for the clean surface.

We have reported above that WF sites are centered by Mn atoms. A chemically driven adsorption of one adatom atop Mn atoms would also highlight the spatial distribution of this transition metal on terraces. Because Mn atoms are quasiperiodically distributed but of low density, the resulting overlayer should not be dense but fivefold symmetric. This was achieved when adsorbing Si atoms on the fivefold *i*-AlPdMn surface, adatoms that tend to form directional covalent bonds ( $sp^3$  configuration) instead of maximizing the coordination as it would have been the case at DS sites.<sup>90</sup> Moreover, the distribution of these Mn atoms also plays a crucial role and impacts the morphology of the molecular thin film.

When  $C_{60}$  molecules are deposited on the twofold *i*-AlPdMn surface, the molecular distribution at the surface is such that most fullerenes lie at the vertices of a Fibonacci square grid, leading to a quasiperiodic molecular network (a low density overlayer). On the twofold *i*-AlPdMn surface, the terminating layers dissect the pseudo-Mackay clusters such that exposed Mn atoms form a Fibonacci square grid of similar dimensions.<sup>91</sup> Further experimental analysis confirms the molecular bonding at Mn sites where a strong interaction between the electron rich Mn and the electron acceptor  $C_{60}$  is expected.<sup>91</sup>

Contrary to the above system, a dense quasiperiodic  $C_{60}$  overlayer can be grown on the fivefold *i*-AlPdMn surface.<sup>92,93</sup> The preferential nucleations at both DS and WS sites promote the formation of a dense self-organized molecular thin film with long-range quasiperiodic order.<sup>92</sup> The growth relies on a symmetry matching between these local fivefold motifs and the fullerene pentagonal faces. These specific configurations allow for an efficient electron transfer from the substrate to the electron deficient molecular pentagonal face. Once the film completed, molecules at the DS site that lie closer to the surface will be imaged as dim molecules by STM.

Exploring novel surfaces of other quasicrystal families opens new horizons in thin film growth and morphology. This has been recently verified when considering Tsai-type quasicrystals (here, *i*-AgInYb) as new templates. The bulk structure is best described as an aperiodic arrangement of rhombic triacontrahedral (RTH) clusters consisting of five concentric atomic shells, which encompass for 93.8% of the atoms. The fivefold *i*-AgInYb surface is formed at dense Yb rich bulk planes intersecting the center of the RTH entities. Such a cut through the building units generates a complex structure where In/Ag and Yb decagonal rings along with Yb pentagons of various sizes are the most striking motifs [Fig. 3(c)].<sup>69</sup> While Pb and Bi form a flat quasiperiodic monolayer on the fivefold *i*-AlPdMn surface, the same elements adopt a quasiperiodic order in several layers of low density on the fivefold *i*-AgInYb.<sup>94,95</sup> Upon adsorption, these elements are sequentially positioned on the surface at vacant sites normally populated by atoms present in the intact RTH cluster. This occurs with the adsorption of Pb adatoms at different heights constituting several adlayers. In this system, the sufficiently short adatom–adatom distances compared to bulk Pb suggest a strong interaction between adatoms. Moreover, the adlayer–adlayer interaction is crucial to stabilize the formation of the 3D growth of quasicrystalline Pb. This study also highlights the importance of the adsorption order toward the 3D quasicrystalline formation.<sup>94</sup>

The adsorption of Bi atoms on the fivefold *i*-AgInYb<sup>95</sup> leads to a comparable 3D quasicrystalline structure. However, the growth mechanism is somehow different with the coexistence of Bi crescents and pentagons at low coverage, whereas only pentagonal islands are observed for the Pb adatoms. Moreover, the order in the adsorption of the layers differs between the two systems. Nevertheless, Bi adatoms will also grow in layers of different heights and adsorption energies to *in fine* occupy the atomic positions of the RTH cluster. Can an identical 3D structure be formed on other quasicrystal surfaces? Although only few other orientations have been tested so far, Pb adsorption on threefold *i*-AgInYb<sup>96</sup> can also be explained by filling bulk vacant sites, resulting from the surface truncation. However, the growth mode is altered here due to a much lower atomic density per threefold plane and a greater number of planes per nm in *z* compared to the fivefold surfaces. The consequence on the film morphology is a much more pronounced perpendicular growth to the surface due to less available adsorption sites on the template.<sup>96</sup>

The atypical structural motifs and chemical distribution at the fivefold *i*-AgInYb surface have been shown to also impact the growth of the pentacene (Pn) thin film.<sup>93</sup> The rod-shaped molecules consist of five acene rings fused along C–C bonds. The molecules, imaged by STM as four-lobed features, nucleate at quasiperiodic sites, hence creating a quasiperiodic molecular ordering. From the twofold symmetry of the molecules, which limits the possible bonding configurations to the substrate combined with the analysis of the molecular orientations and locations, the adsorption sites are identified as tenfold symmetric points around RTH clusters. More precisely, Pn molecules will interact with the substrate via the formation of two bonds, each between a terminal Pn benzene ring and a substrate Yb atom.<sup>93</sup>

On the same substrate, symmetry matching between Yb pentagons and RTH cluster centers and other molecules, here, the fivefold symmetric corannulene molecules ( $C_{20}H_{10}$ ), enforces long-range periodic order in the molecular films. The molecules with their bowl-openings pointing away from the surface self-assemble

into decagonal rings, recurrent motif identified within the overlayer. However, due to steric hindrance, these adsorption sites could not be populated simultaneously, which translated into an aperiodic thin film of low density.<sup>86</sup>

Recently, the realization of a metastable Sn quasicrystalline clathrate on the fivefold *i*-AlPdMn surface has once more highlighted the impact of a complex adsorption landscape for the discovery of novel nano-scale architectures and new phases.<sup>87</sup> At the early stage of the nucleation, Sn adatoms self-assemble into ten-atom starfish clusters atop WF sites (as for the Pb element). The formation of these pentagonal islands is crucial for the formation of the quasiperiodic overlayer. More importantly, the starfish configuration is a part of the clathrate structure reported here [Fig. 3(d)]. The inner Sn pentagons match the top pentagonal faces of the dodecahedron present in the clathrate structure. In addition, the coincidence between the cage–cage linkage lengths in the Sn clathrate with the WF-to-WF separations on fivefold *i*-AlPdMn is what makes the growth of the Sn clathrate feasible.<sup>87</sup> This interface compatibility prevents the formation of more stable crystalline structures and promotes the quasiperiodic ordering of thick layer of elemental Sn on the quasicrystal fivefold surface. The impact of the fivefold *i*-AlPdMn surface on the morphology of an elemental thick film was originally demonstrated for Cu and Co adsorptions. However, the corresponding film structures were drastically different from the Sn clathrate and understood as quasiperiodically modulated multilayer structures.<sup>97,98</sup>

The above examples demonstrate how the structurally and chemically complex elementary clusters once truncated at the surface influence the growth mode and morphology of thin films. For polar intermetallics such as Al<sub>13</sub>TM<sub>4</sub> quasicrystal approximants, the influence of the substrate remains important on the elemental and molecular adsorption mechanism. As opposed to Al-based quasicrystal surfaces, the surface terminations can be flat or highly corrugated depending on whether the bulk clusters are preserved intact or dissected when exposed at the surface. For the highly corrugated Al<sub>13</sub>Fe<sub>4</sub>(010) surface with deep trough and a low atomic density, one could have initially expected the systematic growth of disordered overlayers. However, the adsorption of Pb atoms leads to a pseudomorphic growth as confirmed by LEED and STM analysis. More importantly, the local adatom arrangements tend to replicate the bipentagonal motifs' characteristics of the clean substrate along with a small rumpling.<sup>99</sup>

Similarly, the Pb adsorption study performed on Al<sub>13</sub>Co<sub>4</sub>(100), a flat surface, resulted once more in a pseudomorphic monolayer.<sup>100</sup> High-temperature deposition increases the structural ordering within the film. The structure of the film is composed of irregular Pb pentagons distributed periodically across the terraces. These pentagons are larger than those present on the clean substrate, but they share common vertices with the beneath Al bipentagonal motifs.

Concentrating on molecular adsorption, it is possible that the local fivefold motifs present on the Al<sub>13</sub>Co<sub>4</sub>(100) surface could also act as preferred adsorption sites through symmetry matching for fullerenes, presenting pentagonal carbon faces. In fact, DFT calculations have highlighted two strong adsorption configurations: one with the hexagonal face of the C<sub>60</sub> molecule facing the center of one Al bipentagonal motif located slightly below the mean position of the surface plane and a second with, indeed, the pentagonal C<sub>60</sub> face parallel to the surface in between the two sets of Al

bipentagonal motifs.<sup>101</sup> Due to steric considerations, both sites cannot be populated simultaneously, explaining part of the disorder observed in the molecular film. For high-temperature deposition and low coverage, the fullerenes gather into elongated islands aligned in specific directions, which alternate on adjacent terraces. This anisotropic growth is dictated by the orientation of the bipentagonal motifs present on the clean substrate, which appear rotated on consecutive terraces due to symmetry element. Once completed, the quasi-ordered and rumpled C<sub>60</sub> film adopts the orthorhombic unit mesh of the substrate.<sup>101</sup>

## CONCLUSION

In this paper, we reviewed the basic concepts related to the exploitation of the cluster-based bulk structure of complex intermetallic compounds—quasicrystals and related phases—to design surfaces with specific morphologies. We have shown that bulk cages are not systematically kept intact at the surface and that surface morphologies are mostly governed by both the intrinsic electronic structure of the compounds and the surface preparation conditions. The remarkable properties of complex intermetallic nanostructures are not yet intensively exploited, but a few of them already show promising catalytic properties.<sup>102–105</sup> The design of specific combinations of host–guest cage structures<sup>106</sup> would open the door to the design of surfaces with tunable morphologies for surface-related applications, such as optical properties, or 2D quasiperiodic magnetic systems through ordering of magnetic molecules.

Thin films, resulting from the arrangement of atomic or molecular building blocks at the surface, can further modify the surface morphologies. Here, again, the bulk cage structure impacts the film morphologies. The complex potential energy landscape of the substrate controls the growth and ordering, while the molecular film arrangements can be tuned by the molecule-adsorption site symmetry and size matching.

Until now, only a very small number of cluster-based intermetallic surfaces have been investigated; thus, many of them remain to be explored.

## DEDICATION

In the memory of Pat Thiel, a kind-hearted person who paved the way for so many scientists.

## ACKNOWLEDGMENTS

This work was supported by the European Integrated Center for the Development of New Metallic Alloys and Compounds. E.G. acknowledges financial support through the COMETE project (COnception *in silico* de Matériaux pour l'Environnement et l'Énergie) co-funded by the European Union under the program FEDER-FSE Lorraine et Massif des Vosges 2014–2020. This work was granted access to the HPC resources of TGCC, CINES, and IDRIS under the allocation 99642 attributed by the GENCI (Grand Equipement National de Calcul Intensif). High performance computing resources were also partially provided by the EXPLOR center hosted by the University de Lorraine (Project No. 2017M4XXX0108).

## DATA AVAILABILITY

Data sharing is not applicable to this article as no new data were created or analyzed in this study.

## REFERENCES

- <sup>1</sup>M. A. V. Hove, R. Koestner, P. C. Stair, J. P. Biberian, L. L. Kesmodel, I. Bartos, and G. A. Somorjai, "The surface reconstructions of the (100) crystal faces of iridium, platinum and gold: I. Experimental observations and possible structural models," *Surf. Sci.* **103**, 189 (1981).
- <sup>2</sup>G. A. Somorjai and M. A. van Hove, "Adsorbate-induced restructuring of surfaces," *Prog. Surf. Sci.* **30**, 201–231 (1989).
- <sup>3</sup>V. Fiorentini, M. Methfessel, and M. Scheffler, "Reconstruction mechanism of fcc transition metal (001) surfaces," *Phys. Rev. Lett.* **71**, 1051–1054 (1993).
- <sup>4</sup>W. Moritz and D. Wolf, "Structure determination of the reconstructed Au(110) surface," *Surf. Sci.* **88**, L29–L34 (1979).
- <sup>5</sup>D. L. Adams, H. B. Nielsen, M. A. Van Hove, and A. Ignatiev, "LEED study of the Pt(110)-(1 × 2) surface," *Surf. Sci.* **104**, 47–62 (1981).
- <sup>6</sup>C.-M. Chan, M. A. van Hove, W. H. Weinberg, and E. D. Williams, "Structural study of the reconstructed Ir(110)-(1 × 2) surface by low-energy electron diffraction," *Solid State Commun.* **30**, 47–49 (1979).
- <sup>7</sup>M. K. Debe and D. A. King, "Space-group determination of the low-temperature W001( $\sqrt{2} \times \sqrt{2}$ )R45° surface structure by low-energy-electron diffraction," *Phys. Rev. Lett.* **39**, 708–711 (1977).
- <sup>8</sup>E. H. Conrad, "Surface roughening, melting, and faceting," *Prog. Surf. Sci.* **39**, 65–116 (1992).
- <sup>9</sup>J. E. Y. Jin, Y. Deng, W. Zuo, X. Zhao, D. Han, Q. Peng, and Z. Zhang, "Wetting models and working mechanisms of typical surfaces existing in nature and their application on superhydrophobic surfaces: A review," *Adv. Mater. Interfaces* **5**, 1701052 (2018).
- <sup>10</sup>J. H. Morkkath, "Shapes matter: Examining the optical response evolution in stretched aluminium nanoparticles via time-dependent density functional theory," *Phys. Chem. Chem. Phys.* **20**, 51 (2018).
- <sup>11</sup>L. Yuan, M. Lou, B. D. Clark, M. Lou, L. Zhou, S. Tian, C. R. Jacobson, P. Nordlander, and N. J. Halas, "Morphology-Dependent reactivity of a plasmonic photocatalyst," *ACS Nano* **14**, 12054–12063 (2020).
- <sup>12</sup>S. Kühl, M. Gocyla, H. Heyen, S. Selve, M. Heggen, R. E. Dunin-Borkowski, and P. Strasser, "Concave curvature facets benefit oxygen electroreduction catalysis on octahedral shaped PtNi nanocatalysts," *J. Mater. Chem. A* **7**, 1149–1159 (2019).
- <sup>13</sup>H. B. Bohidar and K. Rawat, *Design of Nanostructures: Self-Assembly of Nano-materials*, John Wiley & Sons, 2017.
- <sup>14</sup>M. Beilstein, *J. Nanotechnol.* **6**, 1397–1398 (2015).
- <sup>15</sup>C. Tan, X. Cao, X.-J. Wu, Q. He, J. Yang, X. Zhang, J. Chen, W. Zhao, S. Han, G.-H. Nam *et al.*, "Recent advances in ultrathin two-dimensional nanomaterials," *Chem. Rev.* **117**, 6225–6331 (2017).
- <sup>16</sup>M. Schwarz, A. Riss, M. Garnica, J. Ducke, P. S. Deimel, D. A. Duncan, P. K. Thakur, T.-L. Lee, A. P. Seitsonen, J. V. Barth *et al.*, "Corrugation in the weakly interacting hexagonal-BN/Cu(111) system: Structure determination by combining noncontact atomic force microscopy and X-ray standing waves," *ACS Nano* **11**, 9151–9161 (2017).
- <sup>17</sup>A. Belsky, M. Hellenbrandt, V. L. Karen, and P. Luksch, "New developments in the inorganic crystal structure Database (ICSD): Accessibility in support of materials research and design," *Acta Crystallogr., Sect. B* **58**, 364–369 (2002).
- <sup>18</sup>P. Villars and K. Cenzual, *Pearson's Crystal Data: Crystal Structure Database for Inorganic Compounds, Release 2012/13* (ASM International, Materials Park, OH, 2013).
- <sup>19</sup>T. G. Akhmetshina, V. A. Blatov, D. M. Proserpio, and A. P. Shevchenko, "Topology of intermetallic structures: From statistics to rational design," *Acc. Chem. Res.* **51**, 21–30 (2018).
- <sup>20</sup>K. S. Chan, M. A. Miller, and X. Peng, "First-principles computational study of hydrogen storage in silicon clathrates," *Mater. Res. Lett.* **6**, 72–78 (2018).
- <sup>21</sup>M. Hirscher, V. A. Yartys, M. Baricco, J. Bellosta von Colbe, D. Blanchard, R. C. Bowman, D. P. Broom, C. E. Buckley, F. Chang, P. Chen *et al.*, "Materials for hydrogen-based energy storage – past, recent progress and future outlook," *J. Alloys Compd.* **827**, 153548 (2020).
- <sup>22</sup>B. B. Iversen, A. E. C. Palmqvist, D. E. Cox, G. S. Nolas, G. D. Stucky, N. P. Blake, and H. Metiu, "Why are clathrates good candidates for thermoelectric materials?," *J. Solid State Chem.* **149**, 455–458 (2000).
- <sup>23</sup>M. Krajci and J. Hafner, "Semihydrogenation of acetylene on the (010) surface of GaPd<sub>2</sub>: Ga enrichment improves selectivity," *J. Phys. Chem. C* **118**, 12285–12301 (2014).
- <sup>24</sup>P. A. Thiel, "Quasicrystal surfaces," *Annu. Rev. Phys. Chem.* **59**, 129 (2008).
- <sup>25</sup>C. J. Jenks and P. A. Thiel, "Comments on quasicrystals and their potential use as catalysts," *J. Mol. Catal. A: Chem.* **131**, 301–306 (1998).
- <sup>26</sup>V. Blum, L. Hammer, C. Schmidt, O. Wiecehorst, S. Müller, and K. Heinz, "Segregation in strongly ordering compounds: A key role of constitutional defects," *Phys. Rev. Lett.* **89**, 266102 (2002).
- <sup>27</sup>J. Kitchin, K. Reuter, and M. Scheffler, "Alloy surface segregation in reactive environments: First-principles atomistic thermodynamics study of Ag<sub>3</sub>Pd(111) in oxygen atmospheres," *Phys. Rev. B* **77**, 075437 (2008).
- <sup>28</sup>R. Asahi, H. Sato, T. Takeuchi, and U. Mizutani, "Verification of Hume-Rothery electron concentration rule in Cu<sub>5</sub>Zn<sub>8</sub> and Al<sub>3</sub>Cu<sub>9</sub>  $\gamma$  brasses by *ab initio* FLAPW band calculations," *Phys. Rev. B* **71**, 165103 (2005).
- <sup>29</sup>V. A. Rogalev, O. Gröning, R. Widmer, J. H. Dil, F. Bisti, L. L. Lev, T. Schmitt, and V. N. Strocov, "Fermi states and anisotropy of Brillouin zone scattering in the decagonal Al-Ni-Co quasicrystal," *Nat. Commun.* **6**, 8607 (2015).
- <sup>30</sup>R. Ferro and A. Saccone, *Intermetallic Chemistry* (Pergamon Elsevier, Oxford, UK, 2008).
- <sup>31</sup>A. P. Tsai, S. Kameoka, and Y. Ishii, "PdZn=Cu: Can an intermetallic compound replace an element?," *J. Phys. Soc. Jpn.* **73**, 3270–3273 (2004).
- <sup>32</sup>Y. Ishii and T. Fujiwara, "Electronic structure and stability mechanisms of quasicrystals," *Quasicrystals*, Handbook of Metal Physics, edited by Y. Ishii and T. Fujiwara (Elsevier Science, 2008), pp. 171–208.
- <sup>33</sup>N. F. Mott and H. Jones, *The Theory of the Properties of Metals and Alloys* (Dover, 1958).
- <sup>34</sup>C. T. Liu, E. P. George, P. J. Maziasz, and J. H. Schneibel, "Recent advances in B2 iron aluminide alloys: Deformation, fracture and alloy design," *Mater. Sci. Eng. A* **258**, 84 (1998).
- <sup>35</sup>J. Kwon, L. Thuinet, M.-N. Avettand-Fénoël, A. Legris, and R. Besson, "Point defects and formation driving forces of complex metallic alloys: Atomic-scale study of Al<sub>4</sub>Cu<sub>9</sub>," *Intermetallics* **46**, 250–258 (2014).
- <sup>36</sup>T. Duguet, E. Gaudry, T. Deniozou, J. Ledieu, M. C. de Weerd, T. Belmonte, J.-M. Dubois, and V. Fournée, "Complex metallic surface alloys in the Al/Cu(111) system: An experimental and computational study," *Phys. Rev. B* **80**, 205412 (2009).
- <sup>37</sup>E. Gaudry, A. K. Shukla, T. Duguet, J. Ledieu, M.-C. deWeerd, J.-M. Dubois, and V. Fournée, "Structural investigation of the (110) surface of  $\gamma$ -Al<sub>4</sub>Cu<sub>9</sub>," *Phys. Rev. B* **82**, 085411 (2010).
- <sup>38</sup>C. S. Spanjers, A. Dasgupta, M. Kirkham, B. A. Burger, G. Kumar, M. J. Janik, and R. M. Rioux, "Determination of bulk and surface atomic arrangement in Ni-Zn  $\gamma$ -brass phase at different Ni to Zn ratios," *Chem. Mater.* **29**, 504–512 (2017).
- <sup>39</sup>C. Dong, "The  $\delta$ -Al<sub>4</sub>Cu<sub>9</sub> phase as an approximant of quasicrystals," *Philos. Mag. A* **73**, 1519–1528 (1996).
- <sup>40</sup>A. Dasgupta, E. K. Zimmerer, R. J. Meyer, and R. M. Rioux, "Generalized approach for the synthesis of silica supported Pd-Zn, Cu-Zn and Ni-Zn gamma brass phase nanoparticles," *Catal. Today* **334**, 231–242 (2019).
- <sup>41</sup>J. V. Zaikina, T. Mori, K. Kovnir, D. Teschner, A. Senyshyn, U. Schwarz, Y. Grin, and A. V. Shevelkov, "Bulk and surface structure and high-temperature thermoelectric properties of inverse clathrate-III in the Si-P-Te system," *Chem. - Eur. J.* **16**, 12582–12589 (2010).
- <sup>42</sup>K. Anand, H. D. Nguyen, M. Baitinger, C. Allio, C. Krellner, Y. Grin, J. Ledieu, V. Fournée, and É. Gaudry, "Ba<sub>8</sub>Au<sub>5.25</sub>Ge<sub>40.75</sub>(110): A nano-caged surface electronically controlled by barium and gold adatoms," *J. Phys. Chem. C* **122**, 29298–29306 (2018).

- <sup>43</sup>K. Anand, C. Allio, C. Krellner, H. D. Nguyen, M. Baitinger, Y. Grin, J. Ledieu, V. Fournée, and É. Gaudry, "Charge balance controls the (100) surface structure of the  $\text{Ba}_8\text{Au}_{5.25}\text{Ge}_{40.75}$  clathrate," *J. Phys. Chem. C* **122**, 2215–2220 (2018).
- <sup>44</sup>P. W. Loscutoff and S. F. Bent, *Annu. Rev. Phys. Chem.* **57**, 467–495 (2006).
- <sup>45</sup>L. Zhang, E. G. Wang, Q. K. Xue, S. B. Zhang, and Z. Zhang, "Generalized electron counting in determination of metal-induced reconstruction of compound semiconductor surfaces," *Phys. Rev. Lett.* **97**, 126103 (2006).
- <sup>46</sup>G. T. de Laissardière, D. N. Manh, and D. Mayou, "Electronic structure of complex Hume-Rothery phases and quasicrystals in transition metal aluminides," *Prog. Mater. Sci.* **50**, 679–788 (2005).
- <sup>47</sup>Y. Takagiwa and K. Kimura, "Metallic-covalent bonding conversion and thermoelectric properties of Al-based icosahedral quasicrystals and approximants," *Sci. Technol. Adv. Mater.* **15**, 044802 (2014).
- <sup>48</sup>P. Scheid, C. Chatelier, J. Ledieu, V. Fournée, and É. Gaudry, "Bonding network and stability of clusters: The case study of the  $\text{Al}_{13}\text{TM}_4$  pseudo-10fold surfaces," *Acta Crystallogr., Sect. A* **75**, 314–324 (2019).
- <sup>49</sup>Q. Lin and G. J. Miller, "Electron-poor polar intermetallics: Complex structures, novel clusters, and intriguing bonding with pronounced electron delocalization," *Acc. Chem. Res.* **51**, 49–58 (2018).
- <sup>50</sup>M. Meier, J. Ledieu, M.-C. D. Weerd, Y.-T. Huang, G. J. P. Abreu, R. Diehl, T. Mazet, V. Fournée, and E. Gaudry, "Interplay between bulk atomic clusters and surface structure in complex intermetallic compounds: The case study of the  $\text{Al}_5\text{Co}_2(001)$  surface," *Phys. Rev. B* **91**, 085414 (2015).
- <sup>51</sup>M. Meier, J. Ledieu, M.-C. D. Weerd, V. Fournée, and E. Gaudry, "Structural investigations of  $\text{Al}_5\text{Co}_2(2\bar{1}0)$  and (100) surfaces: Influence of bonding strength and annealing temperature on surface terminations," *Phys. Rev. B* **93**, 075412 (2016).
- <sup>52</sup>J. Ledieu, E. Gaudry, L. N. S. Loli, S. A. Villaseca, M.-C. de Weerd, M. Hahne, P. Gille, Y. Grin, J.-M. Dubois, and V. Fournée, "Structural investigation of the (010) surface of the  $\text{Al}_{13}\text{Fe}_4$  catalyst," *Phys. Rev. Lett.* **110**, 076102 (2013).
- <sup>53</sup>H. Shin, K. Pussi, É. Gaudry, J. Ledieu, V. Fournée, S. Alarcón-Villaseca, J.-M. Dubois, Y. Grin, P. Gille, W. Moritz *et al.*, "Structure of the orthorhombic  $\text{Al}_{13}\text{Co}_4(100)$  surface using LEED, STM and *ab initio* studies," *Phys. Rev. B* **84**, 085411 (2011).
- <sup>54</sup>E. Gaudry, C. Chatelier, G. McGuirk, L. S. Loli, M.-C. DeWeerd, J. Ledieu, V. Fournée, R. Felici, J. Drnec, G. Beutier *et al.*, "Structure of the  $\text{Al}_{13}\text{Co}_4(100)$  surface: Combination of surface X-ray diffraction and *ab initio* calculations," *Phys. Rev. B* **94**, 165406 (2016).
- <sup>55</sup>J. Ledieu, E. Gaudry, M.-C. de Weerd, R. D. Diehl, and V. Fournée, "The (100) surface of the  $\text{Al}_{13}\text{Co}_4$  quasicrystalline approximant," *Mater. Res. Soc. Symp. Proc.* **1517**, 207 (2012).
- <sup>56</sup>J. Ledieu, É. Gaudry, K. Pussi, T. Jarrin, P. Scheid, P. Gille, and V. Fournée, "Reconstruction of the  $\text{Al}_{13}\text{Ru}_4(010)$  approximant surface leading to anisotropic molecular adsorption," *J. Phys. Chem. C* **121**, 22067–22072 (2017).
- <sup>57</sup>F. Brix, R. Simon, and É. Gaudry, "The (010) surface of the  $\text{Al}_{45}\text{Cr}_7$  complex intermetallic compound: Insights from density functional theory," *Z. Anorg. Allg. Chem.* **646**, 1176–1182 (2020).
- <sup>58</sup>C. Chatelier, Y. Garreau, A. Vlad, J. Ledieu, A. Resta, V. Fournée, M.-C. de Weerd, A. Coati, and E. Gaudry, "The pseudo-twofold surface of the  $\text{Al}_{13}\text{Co}_4$  catalyst: Structure, stability, and hydrogen adsorption," *ACS Appl. Mater. Interfaces* **12**, 39787 (2020).
- <sup>59</sup>F. Abdel-Hamid, M.-C. de Weerd, É. Gaudry, and V. Fournée, "Investigation of the (100) surface of the  $\text{Ce}_3\text{Pd}_{20}\text{Si}_6$  intermetallic cage compound," *J. Phys. Chem. C* **123**, 12355–12366 (2019).
- <sup>60</sup>P. Ebert, M. Feuerbacher, N. Tamura, M. Wollgarten, and K. Urban, "Evidence for a cluster-based structure of  $\text{AlPdMn}$  single quasicrystals," *Phys. Rev. Lett.* **77**, 3827 (1996).
- <sup>61</sup>P. Ebert, F. Yue, and K. Urban, *Phys. Rev. B* **57**, 2821 (1998).
- <sup>62</sup>L. Ponson, D. Bonamy, and L. Barbier, "Cleaved surface of *i*- $\text{AlPdMn}$  quasicrystals: Influence of the local temperature elevation at the crack tip on the fracture surface roughness," *Phys. Rev. B* **74**, 184205 (2006).
- <sup>63</sup>M. Gierer, M. A. Van Hove, A. I. Goldman, Z. Shen, S.-L. Chang, C. J. Jenks, C.-M. Zhang, and P. A. Thiel, "Structural analysis of the fivefold symmetric surface of the  $\text{Al}_{70}\text{Pd}_{21}\text{Mn}_9$  quasicrystal by low energy electron diffraction," *Phys. Rev. Lett.* **78**, 467 (1997).
- <sup>64</sup>Z. Papadopolos, G. Kasner, J. Ledieu, E. J. Cox, N. V. Richardson, Q. Chen, R. D. Diehl, T. A. Lograsso, A. R. Ross, and R. McGrath, "Bulk termination of the quasicrystalline fivefold surface of  $\text{Al}_{70}\text{Pd}_{21}\text{Mn}_9$ ," *Phys. Rev. B* **88**, 184207 (2002).
- <sup>65</sup>L. Barbier, D. L. Floc'h, Y. Calvayrac, and D. Gratias, "Identification of the atomic structure of the fivefold surface of an icosahedral Al-Pd-Mn quasicrystal: Helium diffraction and scanning tunneling microscopy studies," *Phys. Rev. Lett.* **88**, 085506 (2002).
- <sup>66</sup>H. Sharma, K. Franke, W. Theis, A. Riemann, S. Fölsch, P. Gille, and K. Rieder, "Structure and morphology of the tenfold surface of decagonal  $\text{Al}_{71.8}\text{Ni}_{14.8}\text{Co}_{13.4}$  in its low-temperature random tiling type-I modification," *Phys. Rev. B* **70**, 235409 (2004).
- <sup>67</sup>P. A. Thiel, B. Únal, C. J. Jenks, A. I. Goldman, P. C. Canfield, T. A. Lograsso, J. W. Evans, M. Quiquandon, D. Gratias, and M. A. Van Hove, *Isr. J. Chem.* **51**, 1326–1339 (2011).
- <sup>68</sup>J. Ledieu and R. McGrath, "Nanostructured quasiperiodic surfaces: The origin of pentagonal hollows and their role in adsorption and nucleation processes," *J. Phys.: Condens. Matter* **15**, S3113 (2003).
- <sup>69</sup>H. Sharma, M. Shimoda, K. Sagisaka, H. Takakura, J. Smerdon, P. Nugent, R. McGrath, D. Fujita, S. Ohhashi, and A. Tsai, "Structure of the fivefold surface of the Ag-in-Yb icosahedral quasicrystal," *Phys. Rev. B* **80**, 121401 (2009).
- <sup>70</sup>V. Fournée, P. J. Pinhero, J. W. Anderegg, T. A. Lograsso, A. R. Ross, P. C. Canfield, I. R. Fisher, and P. A. Thiel, "Electronic structure of quasicrystalline surfaces: Effects of surface preparation and bulk structure," *Phys. Rev. B* **62**, 14049–14059 (2000).
- <sup>71</sup>V. Fournée, E. Belin-Ferré, P. Pêcheur, J. Tobola, Z. Dankhazi, A. Sadoc, and H. Müller, "Electronic structure of Al-Pd-Mn crystalline and quasicrystalline alloys," *J. Phys.: Condens. Matter* **14**, 87 (2002).
- <sup>72</sup>K. Horn, W. Theis, J. J. Paggel, S. R. Barman, E. Rotenberg, P. Ebert, and K. Urban, "Core and valence level photoemission and photoabsorption study of icosahedral Al-Pd-Mn quasicrystals," *J. Phys.: Condens. Matter* **18**, 435–448 (2006).
- <sup>73</sup>R. Mader, R. Widmer, P. Groning, S. Deloudi, W. Steurer, M. Heggen, P. Schall, M. Feuerbacher, and O. Groning, "High-resolution scanning tunneling microscopy investigation of the (12110) and (10000) two-fold symmetric d-Al-Ni-Co quasicrystalline surfaces," *Phys. Rev. B* **80**, 035433 (2009).
- <sup>74</sup>H. Sharma, W. Theis, P. Gille, and K. Rieder, "Faceting of the two-fold decagonal  $\text{Al}_{71.8}\text{Ni}_{14.8}\text{Co}_{13.4}(0\ 0\ 1\ 1\ 0)$  surface studied by He diffraction."
- <sup>75</sup>A. Mathur, P. Sharma, and R. C. Cammarata, "Negative surface energy - clearing up confusion," *Nat. Mater.* **4**, 186 (2005).
- <sup>76</sup>É. Gaudry, C. Chatelier, D. Loffreda, D. Kandaskalov, A. Coati, and L. Piccolo, "Catalytic activation of a non-noble intermetallic surface through nanostructuring under hydrogenation conditions revealed by atomistic thermodynamics," *J. Mater. Chem. A* **8**, 7422–7431 (2020).
- <sup>77</sup>V. Fournée and P. A. Thiel, "New phenomena in epitaxial growth: Solid films on quasicrystalline substrates," *J. Phys. D: Appl. Phys.* **38**, R83 (2005).
- <sup>78</sup>H. R. Sharma, M. Shimoda, and A. P. Tsai, "Quasicrystal surfaces: Structure and growth of atomic overlayers," *Adv. Phys.* **56**, 403 (2007).
- <sup>79</sup>J. A. Smerdon, L. H. Wearing, J. K. Parle, L. Leung, H. R. Sharma, J. Ledieu, and R. McGrath, "Ordering of adsorbed species on quasicrystal surfaces," *Philos. Mag.* **88**, 2073–2082 (2008).
- <sup>80</sup>J. A. Smerdon, "The various modes of growth of metals on quasicrystals," *J. Phys. Condens. Matter* **22**, 433002 (2010).
- <sup>81</sup>R. McGrath, J. A. Smerdon, H. R. Sharma, W. Theis, and J. Ledieu, "The surface science of quasicrystals," *J. Phys.: Condens. Matter* **22**, 084022 (2010).
- <sup>82</sup>T. Cai, J. Ledieu, R. McGrath, V. Fournée, T. Lograsso, A. Ross, and P. Thiel, "Pseudomorphic starfish: Nucleation of extrinsic metal atoms on a quasicrystalline substrate," *Surf. Sci.* **526**, 115 (2003).
- <sup>83</sup>C. Ghosh, D.-J. Liu, K. J. Schnitzenbaumer, C. J. Jenks, P. A. Thiel, and J. W. Evans, *Surf. Sci.* **600**, 2220 (2006).
- <sup>84</sup>M. Krajčí, J. Hafner, J. Ledieu, and R. McGrath, "*Ab initio* study of quasiperiodic bilayers on a tenfold d-Al-Co-Ni surface," *Phys. Rev. B* **73**, 184202 (2006).
- <sup>85</sup>J. Ledieu, M. Krajčí, J. Hafner, L. Leung, L. Wearing, R. McGrath, T. Lograsso, D. Wu, and V. Fournée, "Nucleation of Pb starfish clusters on the fivefold Al-Pd-Mn quasicrystal surface," *Phys. Rev. B* **79**, 165430 (2009).

- <sup>86</sup>N. Kalashnyk, J. Ledieu, É. Gaudry, C. Cui, A.-P. Tsai, and V. Fournée, "Building 2D quasicrystals from 5-fold symmetric corannulene molecules," *Nano Res.* **11**, 2129–2138 (2018).
- <sup>87</sup>V. K. Singh, M. Mihalkovic, M. Krajci, S. Sarkar, P. Sadhukhan, M. Maniraj, A. Rai, K. Pussi, D. L. Schlagel, T. A. Lograsso *et al.*, "Quasiperiodic ordering in thick Sn layer on *i*-Al-Pd-Mn: A possible quasicrystalline clathrate," *Phys. Rev. Res.* **2**, 013023 (2020).
- <sup>88</sup>J. Ledieu, L. Leung, L. Wearing, R. McGrath, T. Lograsso, D. Wu, and V. Fournée, "Self-assembly, structure, and electronic properties of a quasiperiodic lead monolayer," *Phys. Rev. B* **77**, 073409 (2008).
- <sup>89</sup>J. Smerdon, J. Parle, L. Wearing, T. Lograsso, A. Ross, and R. McGrath, *Phys. Rev. B* **78**, 075407 (2008).
- <sup>90</sup>J. Ledieu, P. Unsworth, T. Lograsso, A. Ross, and R. McGrath, *Phys. Rev. B* **73**, 012204 (2006).
- <sup>91</sup>S. Coates, J. Smerdon, R. McGrath, and H. Sharma, *Nat. Commun.* **9**, 3435 (2018).
- <sup>92</sup>V. Fournée, É. Gaudry, J. Ledieu, M.-C. de Weerd, and T. Lograsso, "Self-organized molecular films with long-range quasiperiodic order," *ACS Nano* **8**, 3646–3653 (2014).
- <sup>93</sup>J. A. Smerdon, K. M. Young, M. Lowe, S. S. Hars, T. P. Yadav, D. Hesp, V. R. Dhanak, A. P. Tsai, H. R. Sharma, and R. McGrath, "Templated quasicrystalline molecular ordering," *Nano Lett.* **14**, 1184–1189 (2014).
- <sup>94</sup>H. R. Sharma, K. Nozawa, J. A. Smerdon, P. J. Nugent, I. McLeod, V. R. Dhanak, M. Shimoda, Y. Ishii, A. P. Tsai, and R. McGrath, "Templated three-dimensional growth of quasicrystalline lead," *Nat. Commun.* **4**, 2715 (2013).
- <sup>95</sup>S. S. Hars, H. R. Sharma, J. A. Smerdon, S. Coates, K. Nozawa, A. P. Tsai, and R. McGrath, "Growth of a bismuth thin film on the five-fold surface of the icosahedral Ag-In-Yb quasicrystal," *Surf. Sci.* **678**, 222–227 (2018).
- <sup>96</sup>S. Coates, S. Thorn, R. McGrath, H. R. Sharma, and A. P. Tsai, "Unique growth mode observed in a Pb thin film on the threefold surface of an *i*-Ag-In-Yb quasicrystal," *Phys. Rev. Mater.* **4**, 026003 (2020).
- <sup>97</sup>J. Ledieu, J.-T. Hoeft, D. Reid, J. Smerdon, R. Diehl, T. Lograsso, A. Ross, and R. McGrath, "Pseudomorphic growth of a single element quasiperiodic ultrathin film on a quasicrystal substrate," *Phys. Rev. Lett.* **92**, 135507 (2004).
- <sup>98</sup>J. A. Smerdon, J. Ledieu, J. T. Hoeft, D. E. Reid, L. H. Wearing, R. D. Diehl, T. A. Lograsso, A. R. Ross, and R. McGrath, *Philos. Mag.* **86**, 841 (2006).
- <sup>99</sup>J. Ledieu, M.-C. de Weerd, M. Hahne, P. Gille, and V. Fournée, "Pseudomorphic growth mode of Pb on the Al<sub>13</sub>Fe<sub>4</sub>(010) approximant surface," *Appl. Surf. Sci.* **356**, 862–867 (2015).
- <sup>100</sup>R. Addou, A. K. Shukla, S. Alarcón Villaseca, É. Gaudry, T. Deniozou, M. Heggen, M. Feuerbacher, R. Widmer, O. Gröning, V. Fournée *et al.*, "Lead adsorption on the Al<sub>13</sub>Co<sub>4</sub> (100) surface: Heterogeneous nucleation and pseudomorphic growth," *New J. Phys.* **13**, 103011 (2011).
- <sup>101</sup>V. Fournée, É. Gaudry, J. Ledieu, M.-C. de Weerd, and R. D. Diehl, "Quasi-ordered C<sub>60</sub> molecular films grown on the pseudo-ten-fold (100) surface of the Al<sub>13</sub>Co<sub>4</sub> quasicrystalline approximant," *J. Phys.: Condens. Matter* **28**, 355001 (2016).
- <sup>102</sup>L. Piccolo, C. Chatelier, M.-C. de Weerd, J. Ledieu, V. Fournée, P. Gille, E. Gaudry, and E. Gaudry, "Catalytic properties of Al<sub>13</sub>TM<sub>4</sub> complex intermetallics: Influence of the transition metal and the surface orientation on butadiene hydrogenation," *Sci. Tech. Adv. Mater.* **20**, 557–567 (2019).
- <sup>103</sup>L. Piccolo, L. Kibis, M.-C. De Weerd, E. Gaudry, J. Ledieu, and V. Fournée, "Intermetallic compounds as potential alternatives to noble metals in heterogeneous catalysis: The partial hydrogenation of butadiene on Al<sub>4</sub>Cu<sub>9</sub>(110)," *Chem-CatChem* **9**, 2292–2296 (2017).
- <sup>104</sup>L. Piccolo and L. Kibis, "The partial hydrogenation of butadiene over Al<sub>13</sub>Fe<sub>4</sub>: A surface-science study of reaction and deactivation mechanisms," *J. Catal.* **332**, 112 (2015).
- <sup>105</sup>L. Piccolo, "Al<sub>13</sub>Fe<sub>4</sub> selectively catalyzes the hydrogenation of butadiene at room temperature," *Chem. Commun.* **49**, 9149–9151 (2013).
- <sup>106</sup>J. Wang, Y. He, N. E. Mordvinova, O. I. Lebedev, and K. Kovnir, "The smaller the better: Hosting trivalent rare-earth guests in Cu–P clathrate cages," *Chem* **4**, 1465–1475 (2018).